EUROPEAN COMMISSION
JOINT RESEARCH CENTRE

Institute for Environment and Sustainability

INLAND & MARINE WATERS

DEFINITION OF AN EMPIRICAL INDEX FOR DUST AEROSOL REMOTE SENSING OVER THE MEDITERRANEAN SEA: APPLICATION TO SEAWIFS DATA.

N. Martiny, N. Hoepffner

Integrated Scientific Area 2.2.2
Monitoring and assessing ecosystem variability

ACTION # 2223 '*Monitoring the marine ecosystem variability*'

Dust event crossing Mediterranean Sea on February 5, 2003.

2003 **EUR 20663 EN**

LEGAL NOTICE

A great deal of additional information on the
European Union is available on the Internet.
It can be accessed through the Europa server
(http://europa.eu.int)

EUR 20663 EN

Printed in Italy

Table of contents

Abstract

An empirical index for remote sensing of desert aerosols over the Mediterranean Sea has been defined using the SeaWiFS data archive. The goal of this exercise is twofold:
First, we want to study the desert aerosols, the so-called "dust", in terms of source, repartition, quantity and seasonability over the Mediterranean Sea in order to build a dust climatology.
Second, we want to use this knowledge to make dust deposition models run and evaluate the impact of dust particles on the biogeochemical cycle in the Mediterranean Sea.
In this report, we present the first part of the work, that is the development of a dust aerosol climatology over the Mediterranean Sea. For that purpose, we used the REMBRANDT (REtrieval of Marine Biological Resources through ANalysis of ocean colour DaTa) software (Mélin et al., 2000) as a processing for the SeaWiFS data over the Mediterranean Sea. As this scheme is dedicated to the ocean colour products derivation, dust aerosol zones are commonly flagged through the processing to avoid bad atmospheric corrections. Removing these flags required the development of a parallel process in the REMBRANDT code. The satellite-derived atmospheric signal for any sea pixel at any wavelength is used to define two optical parameters, which are fully described in the report. Series of empirical criteria were applied using these parameters so as to discriminate dust from other aerosols and cirrus. We processed about 140 SeaWiFS images over the Mediterranean Sea from 1998 to 2001 applying those criteria. The results were validated through a match-up analysis with SeaWiFS true-colour browse images. In a second part of the report, we present the preliminary results dealing with the dust climatology. The SeaWiFS dust archive over the Mediterranean Sea extends between 1998 and 2001.

1 *Introduction*

Aerosol coming from deserts or arid zones, commonly named "dust", has been recognized as an important constituent of the atmosphere. On a global scale it has been shown that dust can affect the radiative properties of the atmosphere (Tegen et al., 1997), and indirectly the climate. Moreover as dust can be carried out on long-range scales (Li-Jones & Prospero, 1998), it can be a non negligible source of minerals and associated nutrients (Prospero et al., 2001) to stimulate the oceanic biogeochemical cycles.

To better characterize these global phenomena, an ideal tool to be used is satellite remote sensing techniques and many studies dedicated to the identification of dust from space have been recently developed. For example, the Advanced Very High Resolution Radiometer (AVHRR) algorithm provides a dust aerosol optical thickness (Husar et al., 1997) and the Total Ozone Mapping Spectrometer (TOMS) sensor an index for absorbing aerosols (Herman et al., 1997). Moreover, the plumes can be easily observed from meteorological geostationary satellites such as GOES and METEOSAT (Karayampudi et al., 1999) and ocean color sensors such as the Moderate Resolution Imaging Spectroradiometer (MODIS) and the Sea-viewing Wide-Field-of-view Sensor (SeaWiFS).

Recently, Hsu et al. (2000) adapted the TOMS absorbing aerosol index for the SeaWiFS data. This index is defined from the 412 and 490 nm remote sensing reflectance and describes absorbing aerosols with positive values and non-absorbing particles with negative values. Moreover, the aerosol index is linearly proportional to the aerosol optical thickness, what allows a quantification of the particles. A validation of the index is being done and at the moment only a theoretical description of the method is provided in the literature.

The indirect goal of the study presented here is to highlight the impact of the dust deposition on the oceanic activity. The report deals with the first step of the study: identification of dust from space. For that purpose, we used the SeaWiFS database already available at the Inland and Marine Water unit from the launch of the sensor in September 1997 to December 2001. The SeaWiFS data are processed with the REtrieval of Marine Biological Resources through ANalysis of ocean colour DaTa (REMBRANDT) software (Mélin et al., 2000). This in-house code is specifically dedicated to the derivation of ocean colour products and for that reason, the atmospheric corrections are not derived in cases when the atmospheric reflectance are too high such as with clouds and dust aerosols considered as bright surface over waters. In the REMBRANDT code, we thus created a parallel process to remove the inadequate flags and create a new classification so as to distinguish clouds from dust and dust from other aerosols. We describe in this report the pixel-by-pixel classification we developed, based on the empirical use of two atmospheric optical parameters. In the "Dust" category, we created 4 classes going from the "Dust Storm" (high concentrated ash) to the "Minor Dust Event" (poorly concentrated event).

This work was conducted in the Mediterranean Sea (MED) because this zone bordered by arid and desert zones acts as a major source of crustal aerosols that can be transported largely across the sea in the form of punctual dust events (Guerzoni & Chester, 1996). We applied our pixel classification method to about 140 SeaWiFS images in the years 1998-2001. As a first validation, the resulted spatial patterns were compared to the dust repartition detected at the eye on the SeaWiFS true-colour browses.

In a second part, the 140 processed images were used to study the sources, repartitions and seasonability of the dust aerosols in the MED so as to have a clear idea about the dust spatio-temporal trends in such a zone. This information is indeed important to apply dust deposition models and highlight obvious impacts on the oceanic biological activity.

2 Methodology

2.1 Initial database

First of all, we used the SeaWiFS true-colour browse images to detect visually the dust events. Indeed these ash plumes are usually well detectable at the eye because of their extended geographical coverage (tenth of pixels) and colour aspect (bright yellowish hue). Initially we took into account all the possible dust events, going from the doubtful fine plume particles mixed with clouds to the obvious high concentrated dust event (see Figure 1). Looking at 4 years of SeaWiFS data archive (from 1998 to 2001), we obtained about 300 images.

From this list, we made a second accurate selection, keeping the days for which there was no possible confusion about the dust event. We also eliminated the scenes for which the events, even though clearly observable, were caught in the border of the SeaWiFS image. In that case, the exploitation of the results would not be accurate. As a result, the list was reduced to 140 SeaWiFS images for the entire 4 years period. To cover the full Mediterranean window, we used the raw high-resolution SeaWiFS data recorded at various HRPT stations : HROM (Institute of the Physics of the Atmosphere, Rome, Italy), HSPZ (SACLANT Undersea Research Centre, La Spezia, Italy), HDUN (Dundee University, Scotland, UK), HNEG (Ben-Gurion University of the Negev, Israel) or HMSC (Matera Space Centre, Italy). The exact locations of those stations can be found at the following address: http://daac.gsfc.nasa.gov.

2.2 Exploitation of the selected SeaWiFS data

SeaWiFS data are analysed using an in-house processing code, the REtrieval of Marine Biological Resources through ANalysis of ocean color DaTa (REMBRANDT) software (Mélin et al., 2000). This software has been optimised for the retrieval of biogeochemical parameters at the sea surface and the creation of global maps of these parameters. For example, the mean chlorophyll concentration derived with the REMBRANDT code in the MED from the 21st to 30th of September 1999 is represented in Figure 2.

This operational processing scheme is currently flagging dust aerosols as clouds to avoid any bias in the sea surface products due to inaccurate atmospheric corrections. This point is illustrated in Figure 3. The SeaWiFS browse image of the 27th of October 1999 shows a thick dust event in the Western MED. Once the image is processed with the REMBRANDT code, a major part of the pixels become flagged due to bright surfaces – from either clouds or dust events represented as green and white areas in the image – and to a lesser extent due to bad geometrical conditions -view zenith angles > 56° or solar zenith angles > 70° represented as violet. The non-flagged area is represented in black. In other words, the dust event of the 27th of October 1999 would simply be interpreted as cloudy using the standard satellite processing scheme. To enable the distinction between clouds and dust events, we investigated differences between their optical properties through the analysis of pure atmospheric signals derived from satellite measurements.

2.3 *Differentiation between clouds and dust aerosols*

According to Gordon & Wang (1994), the Top Of Atmosphere (TOA) radiance can be formulated as:

$$L_{toa}=L_{atm}+TL_g+t(L_w+L_{wc}), \quad (1)$$

with:

(i) L_{atm}, the atmospheric radiance,
(ii) L_g, the radiance due to the Fresnel reflection at sea surface attenuated by the atmosphere through the direct transmittance T,
(iii) L_w, the water-leaving radiance attenuated by the atmosphere through the atmospheric diffuse transmittance t,
(iv) L_{wc}, the radiance due to the foam attenuated as well by t.

To evaluate L_{atm} for any pixel (clear sky, clouds, cirrus, dust...) and at any wavelength, it is necessary to determine all the other terms in Eq. (1). First of all, the SeaWiFS sensor is equipped with a tilt system to avoid the glitter contribution (Fraser et al., 1997) so that L_g can be neglected. Second, according to Moore et al. (1998), the derivation of the water-leaving radiance due to the foam L_{wc} can be done knowing the wind speed. The assumptions associated with the estimate of the water-leaving radiances L_w are more subtle. To avoid any discontinuity in the L_w values, we used in all cases the L_w climatology created with the REMBRANDT processing. A large L_w database has indeed been created and maps of averaged L_w are available at http://www.me.sai.jrc.it . For the study, we used 10-days average of L_w over the MED window. In a slightly different way, the transmittances t values were derived from the REMBRANDT code over clear areas and we assumed that the values of diffuse transmittances do not vary over the adjacent flagged zone. Of course, an error budget associated with these hypothesis has to be conducted.

We first derived $L_{atm}(\lambda)$ for 10 SeaWiFS images for which dust events were obvious and we calculated the associated reflectance $\rho_{atm}(\lambda)$ defined as follows:

$$\rho_{atm}=\frac{\pi L_{atm}}{\mu_s E_s}, \quad (2)$$

with μ_s being the cosine of the solar zenith angle and E_s the irradiance at the top of the atmosphere. The signal coming from the aerosols was obtained after correction of the atmospheric reflectance for the Rayleigh component (Gordon et al., 1988). The resulted aerosol reflectance comprises the coupling effects between aerosols and molecules. This preliminary study showed that the reflectance resulting from dust particles can be occasionally as high as the cloud reflectance when the event is thick, especially at 865 nm. Nevertheless, when the concentration is less important (yellow traces on the true-colour browse), the reflectance is always lower than the cloud reflectance, whatever the wavelength. In Figure 4 the aerosol reflectance at 865, 510 and 443 nm are illustrated for the 16th of April 1999. Although a dust event coming from Lybia can be clearly located from the true-colour browse image of that day, the middle of the dust event may be interpreted as a cloud at 865 nm. At 510 nm and 443 nm, the dust event seems less bright than clouds even if the centre of the plume is still as bright as the edge of the cloud detected (represented in red). In other

words, the analysis of the aerosol reflectance alone doesn't enable the discrimination between clouds and dust events.
Nevertheless, a first general test aiming at the removal of the brightest clouds can be applied. For that purpose, we don't use the exact aerosol reflectance but we use the quantity resulting from the subtraction of the Rayleigh contribution from the atmospheric reflectance. This contribution has indeed a much more important weigh comparing to the other terms of Eq. (1). In summary, if this signal is lower than 0.35 at 443 nm (threshold inspired by Gobron et al., 1999), the pixel is bright but not classified as a cloud and may be classified into the dust category.

2.4 Definition of two optical parameters for dust pixel classification

The new pixel classification is based on the optical properties of dust aerosols through the use of two parameters defined from the atmospheric reflectance $\rho_{atm}(\lambda)$.

2.4.1 The f-ratio

The *f*-ratio expresses the change in the atmospheric reflectance when there is addition of absorbing aerosols in the atmosphere. It has been previously used by Antoine & Morel (1999) in the Look-Up-Tables of the European Medium Resolution Imaging Spectrometer (MERIS) algorithm and by Hsu et al. (2000). The so-called *f* parameter is defined as follows:

$$f(\lambda)=\frac{\rho_{atm}(\lambda)}{\rho_r(\lambda)}, \qquad (3)$$

ρ_r being the Rayleigh reflectance. The change in *f* is even more noticeable when the concentration of the aerosols becomes important. To highlight this point, we simulated *f* for different aerosol optical thicknesses τ_a and various geometrical conditions. We used 7 aerosol models, some of them being predefined in the Shettle & Fenn climatology (1979), the others being built from the components described in D'Almeida (1991) and in more recent papers (Kaufman et al., 2002). Table 1 summarizes the characteristics of the aerosol models used for simulations. Among the 7 models, only the Maritime model is non absorbing. The others present more or less absorption, going from the Urban model mostly encountered in the industrial areas to the Major Dust model corresponding to strong dust storms.

Simulations of *f* were done using a radiative transfer code based on the successive order of scattering (Deuzé et al., 1989). 5 visibilities were taken into account: 50 km, 23 km, 8 km, 4 km and 2 km, corresponding respectively to a mean aerosol optical thickness of 0.152, 0.234, 0.520, 0.954 and 1.822 according to the 5S theory (Tanré et al., 1990). The simulations were conducted at 865 nm because of the low value of the Rayleigh reflectance (Rayleigh optical thickness is about 0.0168). The solar zenith angle was set to 30°, view zenith angles going from 30 to 60°.

Figure 5 shows first the increase of the *f*-ratio with turbidity whatever the aerosol model. Second, the magnitude of *f* changes with the absorption in the case of turbid skies. For clear skies, *f* ranges between 1.5 and 3.5 whatever the aerosol model whereas for turbid skies, it can be as great as 20 for the "Major Dust" (most absorbing model) but vary between 10 and 15 for the other absorbing models.

In other words, the *f*-ratio in the near infrared can be used as a discriminator between dust from other aerosols, especially for high concentrated dust episodes.

2.4.2 The ε' parameter

The ε' parameter has been previously defined by Antoine & Morel (1999) as:

$$\varepsilon'(\lambda_1,\lambda_2)=\frac{\rho_{atm}(\lambda_1)-\rho_r(\lambda_1)}{\rho_{atm}(\lambda_2)-\rho_r(\lambda_2)}. \tag{4}$$

$\varepsilon'(\lambda_1,\lambda_2)$ represents the spectral dependency of the aerosol reflectance comprising the multiple scattering effects. Opposite to the ε parameter defined by Gordon & Wang (1994), ε' can be used to distinguish absorbing aerosols from non-absorbing ones, the slope of the spectral dependency of $\varepsilon'(\lambda,865)$ being positive at short wavelengths in the case of weak absorbing aerosols (Antoine & Morel, 1999).

Consequently, the new pixel classification is based on series of tests related to the ε' parameter at short wavelengths. Among them, the values of the slopes β_s and β_l respectively defined as:

$$\beta_s=\frac{\varepsilon'(510,555)-\varepsilon'(412,443)}{\lambda_{green}-\lambda_{blue}}, \tag{5}$$

and:

$$\beta_l=\frac{\varepsilon'(765,865)-\varepsilon'(510,555)}{\lambda_{nir}-\lambda_{green}}, \tag{6}$$

are used as well.

2.5 Empirical criteria for dust pixel classification

The 10 SeaWiFS images selected initially were processed again in order to derive on a pixel-by-pixel basis the following parameters: $\rho_{atm}(\lambda)$, $f(865)$, $\varepsilon'(412,443)$, $\varepsilon'(510,555)$, $\varepsilon'(765,865)$, β_s and β_l. These parameters were analysed in an attempt to identify empirical criteria for the satellite remote sensing of dust aerosols.

The trends highlight two types of dust particles. Even though the value of $\varepsilon'(412,443)$ is always lower than 0.9, the values of $\varepsilon'(510,555)$, β_s and β_l help making the differentiation between both types (see Table 2).

Those optical differences were interpreted using the knowledge of the composition and transport of dust particles. As mentioned by Tegen & Lacis (1996), the uplifted dust particles are composed of sand (particles radius larger than 25 μm), silt (particles radius between 1 and 25 μm) and clay (particles radius smaller than 1 μm). Since the atmospheric lifetime of particles larger than 10 μm is less than one day, the sand and a part of the silt fall down during the transport of the dust due to their size and associated weigh. In other words, the size

distribution of dust particles may be different just after the emission (thus close from the source) and a while after the emission (already far from the source). This phenomena may imply the differences noticed in the values of $\varepsilon'(510,555)$, β_s and β_l so that one category may correspond to dust containing still sand and silt whereas the other category may correspond to particles smaller than 10 µm. The former particles can flow between 7 and 9 days and as they are light, they fall down through a wet deposition process.

Matching those comments with the visible SeaWiFS browse images, the first category defined in Table 2 was assumed to correspond to large dust particles (dark yellow on the images) and the second category to fine dust particles (diffuse yellow colour on the images).

Those properties were correlated to the aerosol concentration through the f-ratio (see Figure 5 showing the relationship between f and τ_a). It came out that the greatest value of f corresponds only to dust category number 1. The intermediary values of f can correspond either to category 1 or 2. The lower value of f corresponds only to category 2. We split thus each of the initial dust categories (see Table 2) into 2 of them (see Table 3). The empirical features of the background aerosols over the sea are specified as class 3.

The pixel classification criteria were defined using only 10 test images. In the following, tests were applied to the whole dataset previously selected, that is to say about 140 SeaWiFS images from 1998 to 2001 included.

To illustrate the previously defined empirical criteria, we chose two days among the 140 processed days and we analysed the $f(865)$, $\varepsilon'(410,443)$, $\varepsilon'(510,555)$, β_s and β_l parameters along adequate transects. The 10th of April 2000 is representative of a dust storm (see Figure 6). The selected transect, drawn in red, goes from the middle of the dust event (dark pink area) to apparently non-contaminated dust area (in black) and crosses the 4 classes of dust particles previously defined in Table 3 (see Figure 7). For the dust class 1a, $f(865)$ is greater than 19, $\varepsilon'(410,443)$ is lower than 0.8 and $\varepsilon'(510,555)$ is lower than 0.95. For the dust class 1b, $f(865)$ ranges between 11 and 18, $\varepsilon'(410,443)$ is lower than 0.85 and $\varepsilon'(510,555)$ varies between 0.95 and 1.05. For the dust class 2a, $f(865)$ is around 10, $\varepsilon'(410,443)$ is lower than 0.9 and $\varepsilon'(510,555)$ is about 1.05. For the dust class 2b, $f(865)$ ranges between 6 and 9, $\varepsilon'(410,443)$ is lower than 0.9 and $\varepsilon'(510,555)$ varies between 1.05 and 1.08. It seems that the results fit our criteria on condition that we include uncertainties. We evaluated the uncertainty on $f(865)$ to be ± 1 and the uncertainty on $\varepsilon'(510,555)$ to be ± to 0.02. No uncertainty on $\varepsilon'(410,443)$ was introduced because the criteria seem to be always fulfilled. We also analysed the β_s and β_l slopes but they do not follow the criteria we defined because of their stability along the transect. As a consequence, the black area next to the dust event observable on the 10th of April 2000 does not correspond neither to a dust zone nor to a background aerosol area. This is not surprising as the dust event is thick on that day and as dust particles may have mixed with other aerosols along such a long distance across the MED.
The 5th of October 2000 was selected to illustrate the background aerosol optical characteristics (class 3 of aerosols in Table 3). Along the transect drawn in red in Figure 8, the slope at short wavelengths β_s is in mean equal to 0.2 in the dust area and in mean equal to 1.5 in the non-contaminated zone (see Figure 9a). The difference between dust and background situation is here easily pointed out. The other slope β_l is in mean equal to 0.85 in the dust area and decreases suddenly in the non-contaminated zone to 0.3 (see Figure 9b). As a result, the boundary between dust and background aerosol situation is generally obvious using the slope parameters.

The empirical criteria defined in Table 3 show thus consistent trends and a good agreement between the new pixel classification and SeaWiFS browse images is obtained. For instance, in Figure 10, a very intensive dust storm coming from Lybia is observable on the 17th of April 2001 SeaWiFS browse image recorded at the HROM station. In Figure 11, a less concentrated dust event crossing the MED is observable on the 26th of March 2001 SeaWiFS browse image recorded at the HROM station. In Figure 12, an ash event in the middle of clouds can be guessed on the 30th of May 1999 SeaWiFS browse image recorded at the HSPZ station.

For the entire database processing, we applied a Mediterranean Sea mask so that the part of the image related to the MED alone is reported. The area outside the mask is represented in white as well as clouds. The land appears in dark green. According to the new pixel classification, class 1a of dust aerosols is represented in dark pink, class 1b in orange, class 2a in yellow, class 2b in clear green and class 3 in black.

In summary, the proposed new pixel classification implemented in the REMBRANDT software enables:

i. to distinguish clouds from dust particles
ii. to quantify dust particles through the *f*-ratio
iii. to detect the spatial repartition of the dust events whatever the concentrations of the events
iv. to distinguish between dust aerosols freshly emitted and the others.

3 Application: dust aerosol climatology over the MED

3.1 Identification of the main sources of dust production

To identify the main sources of desert aerosols production, we used both the results of the new pixel classification (repartition over water) as well as the TOA reflectance measured in the blue (identification over land) by SeaWiFS. Nevertheless, dust zone emission is not always easy to identify, either because of clouds or because of particles that are already crossing the MED. Fortunately, in that case the event can often be related to a previous dust event few days before. At last, meteorological information related to the direction and speed of the wind will be helpful to complete this study. Even though the identification of dust sources is not an easy task, the preliminary results are quite satisfactory and the 4 main sources of Saharan dust found out are in agreement with D'Almeida (1986) and Guerzoni et al. (1996).
Using the 140 SeaWiFS images processed from 1998 to 2001 over the MED, the main sources of desert aerosols are identified in Figure 13 as Morocco/North Mauritania (source 1), South Algeria/Mali/Niger (source 2), South Lybia/Chad (source 3), Egypt/North Sudan (source 4).

3.2 Spatial trends of dust emissions

The frequency of dust events were analysed per zone. To realize the classification, we took into account the duration of the events because those can last from 1 to 5 consecutive days with a statistical distribution as follows: 1 day, 81%; 2 days, 13%; 3 days, 5%; 4 days, 0.8%; 5 days, 0.2% according to Ganor & Foner (1996). A 5-days event counted for 1 in our classification.

The number of annual dust episodes varied between 5 and 35 with an average of 19 in the 1991 but as shown by Ganor & Foner (1996), the annual number of dust episodes is increasing with time (in mean, 10 events a year in 1958 whereas 19 in 1991). For the 1998-2001 period, 26 dust episodes were found out taking into account high and low concentrated events.

Whatever the year, sources 2 and 3 are the most productive among the 4 sources defined in §3.1 (see Figure 14). Source 1 is actually an important source of dust but the emitted particles are generally flowing towards the Atlantic Ocean. Source 4 emits more towards the Eastern direction and consequently towards the land of Israel. Source 4 is generally classified as a A1 type and the sources 2 and 3 as a A2 type (Ganor et al., 1991). Type A storms are usually associated with a cold front with a significant downward flowing jet stream, often accompanied by rain (Alpert & Ganor, 1993). The difference between A1 and A2 type is related to the influence of the sea. Type A1 storms are indeed defined as events passing over only a small portion of the MED whereas type A2 storms are defined as events influenced by marine particles, coated with sea salts and anthropogenic sulphates (Levin et al., 1995).

In sum, Western and Eastern sources are not supposed to produce the same flow of particles. This differentiation can be illustrated by the fact that dust transported to the Eastern MED is mainly deposited by dry deposition while in the Western MED wet deposition is dominant (Molinari, 1996).

3.3 Seasonability of the dust episodes

The frequency of the events was analysed according to the season. An average of the number of events per month using the 4 years of selected data was done (see Figure 15). The most active months are during Spring (from March to May) with a mean number of events/month of 3.5. Summer is quite active with a mean of 3 events/month in July and August. September and October present in mean 2.5 dust events/month, what is not negligible. In this study, the colder months (November, December, January and February) are less active in term of dust production. Figure 16 summarizes the dust activity with the season: the maximum is observed in Spring and the minimum in Winter.

Separating the sources into a Western part (sources 1 and 2) and a Eastern part (sources 3 and 4), it came out that West is much more productive than East (see Figure 17). This could be in disagreement with Figure 14, where sources 2 and 3 were identified as the most productive. Nevertheless, when we combine the number of events of sources 1 and 2 and compare to the number of events of sources 3 and 4, the results are coherent.

A seasonal study reported in Figure 18 shows that Eastern sources are more active in Spring with a mean number of events of 4.5 whereas Western sources are active all year long except

in Winter. A maximum is thus reached in Summer with an average of 7 events/month in June, July and August whereas a minimum of 1 event/month is observed for the whole Winter.

A dust emission seasonability seems to be obviously highlighted using the SeaWiFS database from 1998 to 2001 included. Moreover, the Western and the Eastern parts of the MED are not active at the same period of the year. To check the assumed trends, the SeaWiFS dust database is now being completed with the 2002 data.

Of course, the link between the source of dust and the location of the desert particles over the sea may not be easy to establish. Nevertheless, previous referenced calculations showed that 260 millions tons of dust per year were transported across the northern borders of the Sahara into the West MED (Shutz, 1989) whereas 70 millions of tons were transported into the East MED (Ganor & Mamane, 1982), as reported by Grigoryan & Erdman (1996). To this extent, one can think that most of dust emissions from the Western (Eastern) sources suggest deposition into the West MED (East MED). To complete this study, meteorological database related to wind would be useful so as to investigate the possible trajectory of Saharan dust particles.

4 Conclusion

On a long term basis, this study aims at highlighting the impact of dust aerosols deposition on the oceanic activity. In this report, we present the upstream work, that is to say the detection of dust aerosols from space to study their repartition on a synoptic point of view and develop a dust climatology. The study was conducted using the SeaWiFS database from 1998 to 2001 over the Mediterranean Sea (MED), database processed with the REtrieval of Marine Biological Resources through ANalysis of ocean colour DaTa (REMBRANDT) software (Mélin et al., 2000). This code is specifically dedicated to the ocean colour products derivation and high atmospheric reflectance areas are currently flagged as clouds in order to avoid bad atmospheric corrections. As dust plumes are high atmospheric reflectance areas, they are flagged as clouds.
The first part of this report deals with a description of the modifications brought in the REMBRANDT processing: removal of the initial flags and replacement by others specifically adapted to dust aerosols remote sensing.
First, the threshold of clouds detection is raised to 0.45 in order to flag only the brightest clouds and let the dust pixels in the processing.
Second, empirical criteria are investigated for the creation of new flags. Those criteria are based on two optical parameters defined by Antoine & Morel (1999). The f-ratio defined as the report between the atmospheric and the Rayleigh reflectance expresses the change in the atmospheric reflectance when there is addition of absorbing aerosols in the atmosphere. As f increases with the absorption of aerosols and the aerosol optical thickness it was used: (i) as a discriminator between dust areas and non-contaminated dust areas, (ii) as a discriminator between low concentrated dust event and high concentrated dust storm. The second parameter used for the new flags is the ε' parameter defined as the spectral dependency of the aerosol reflectance comprising the multiple scattering effects (Antoine & Morel, 1999). As the spectral behaviour of ε' changes when there is occurrence of absorbing aerosol, it was used as a discriminator between dust and non-dust areas. Moreover, in the dust pixels, ε' can have two different spectral behaviours that we associated to differences in aerosol size distributions. Particles indeed freshly emitted and close to their source are still composed of

sand, silt and clay whereas the others emitted few days before and thus already far away from their source are composed of silt and clay and are smaller than 10 μm of radius.
The new pixel classification allows to distinguish 6 types of particles: the brightest clouds, the dust storm with large particles, the major dust event with large particles, the major dust event with fine particles, the minor dust event with fine particles and the background situation over the sea or maritime particles.
The new pixel classification was applied to a SeaWiFS dataset of 140 images where all kind of dust events could be observed, from the low to the high concentrated ash plume. The results were compared to SeaWiFS true-colour browse images as a first validation. The agreement is quite satisfactory and gives coherent repartition of dust events over the MED. To conduct a more rigorous validation we plan to use this large dust database for match-up analyses with METEOSAT data (future work with Jean Verdebout, Joint Research Centre, Strategy and System for Space Application Unit).
The second part of the report presents the preliminary results of the dust climatology over the MED using the method previously described. The potential dust sources are firstly identified using the new pixel classification (over waters) as well as the TOA reflectance in the blue (over lands). The 4 main sources found out are in agreement with literature (D'Almeida, 1986; Guerzoni et al., 1996): source 1 being Morocco/North Mauritania, source 2 South Algeria/Mali/Niger; source 3 South Lybia/Chad and source 4 Egypt/South Sudan. The Western sources (1 and 2 together) are systematically more productive than the Eastern sources (3 and 4). As a seasonal pattern, Western sources are productive all year long with a maximum in Summer (average of 7 events/month) and a minimum in Winter (average of 1 event/month) whereas Eastern sources are more productive in spring with a mean of 4.5 events/month. This assessment is in agreement with previous studies (Ganor & Mamane (1982), Shutz (1989), Molinari (1996)).
The link between sources of dust particles and their location over the MED is not obvious and a wind database would be useful to complete this study. Anyway, according to literature (Grigoryan & Erdman, 1996), the input of Saharan dust particles in the West MED is more important than in the East MED, what makes closer the link between the zone of emission and the location of particles over the sea.
The on-going and future work deals with an accurate quantification of dust events over the MED in terms of aerosol optical thickness and fluxes, to be used as inputs of a dust deposition model. To that extent, the dust deposition and marine productivity may be linked through the nutrients brought at the sea surface and ocean colour products such as for instance chlorophyll concentrations.

References

Alpert P. and E. Ganor, "A jet stream associated heavy dust storm in the Western Mediterranean", J. Geophys. Res. 98 (D4), 7339-7349, 1993

Antoine D. and A. Morel, "A multiple scattering algorithm for atmospheric correction of remotely sensed ocean color (MERIS instrument): principle and implementation for atmospheres carrying various aerosols including absorbing ones", Int. J. Remote Sensing 20 (9), 1875-1916, 1999

D'Almeida G. A., "A model for Saharan dust transport", J. Climate and Appl. Meteorol. 25, 903-916, 1986

D'Almeida G. A., P. Koepke and E. P. Shettle, "Atmospheric aerosols global climatology and radiative characteristics", Deepak Publishing, Hampton Virginia USA, 561 pp, 1991

Deuzé J. L., M. Herman, and R. Santer, "Fourier series expansion of the transfer equation in the atmosphere-ocean system", *Journal of Quantitative Spectroscopy and Radiative Transfer*, Vol. 41, No 6, 483-494, 1989

Fraser R. S., S. Mattoo, E. Y. Yeh and C. R. McClain, "Algorithm for atmospheric and glint corrections of satellite measurements of ocean pigment", J. Geophys. Res. 102, 17,107-17,118, 1997

Ganor S. and H. A. Foner, "The mineralogical and chemical properties and the behaviour of aeolian Saharan dust over Israel", S. Guerzoni and R. Chester (eds.), The impact of desert dust across the Mediterranean, Kluwer Academic Publisher, Netherlands, 163-172, 1996

Ganor E., H. A. Foner, S. Brenner, E. Neeman and N. Lavi, "The chemical composition of aerosols settling in Israel following dust storms", Atmos. Environ. 25A, 2665-2670, 1991

Ganor E. and Y. Mamane, "Transport of Saharan Dust Across the Eastern Mediterranean", Atmos. Environ. 16, 581-587, 1982

Gobron N., B. Pinty, M. M. Verstraete and Y. Govaerts, "The MERIS global Vegetation Index (MGVI): description and preliminary application", Int. J. Remote Sensing 20, 1917-1927, 1999

Gordon H. R., J. W. Brown, and R. H. Evans, "Exact Rayleigh scattering calculations for use with the Nimbus-7 coastal zone color scanner", *Appl. Opt.*, 27, 862-871, 1988

Gordon H. R. and M. Wang, "Retrieval of water-leaving radiances and aerosol optical thickness over the oceans with SeaWiFS : a preliminary algorithm", Appl. Opt. 33, (3), 443-452, 1994

Grigoryan S. and L. Erdman, "The preliminary modelling results of Saharan dust transport to the Mediterranean Sea and Europe", S. Guerzoni and R. Chester (eds.), The impact of desert dust across the Mediterranean, Kluwer Academic Publishers, Netherlands, 59-67, 1996

Guerzoni S. and R. Chester, "The impact of desert dust across the Mediterranean", Kluwer Academic Publishers, Netherlands, 1996

Herman J. R., P. K. Barthia, O. Torres, C. Hsu, C. Seftor and E. Celarier, J. Geophys. Res. 102, 16911, 1997

Hsu N. C., W. Robinson, S. W. Bailey, P. J. Werdell, "The description of the SeaWiFS absorbing aerosol index", In S. B. Hooker, & E. R. Firestone, NASA Technical Memorandum 206892, Vol. 10, pp 3-5, Greenbelt, Maryland: NASA Goddard Space Flight Center, 2000

Husar R. B., J. M. Prospero and L. L. Stowe, J. Geophys. Res. 102, 16889, 1997

Karayampudi M. V., S. P. Palm, J. A. Reageb, H. Fang, W. B. Grant, R. M. Hoff, C. Moulin, H. F. Pierce, O. Torres, E. V. Browell and S. H. Melfi, Bull. Amer. Meteorological Soc. 80 (6), 1045, 1999

Kaufman Y. J., D. Tanré and O. Boucher, "A satellite view of aerosols in the climate system", Nature 419, 215-223, 2002

Levin Z., E. Ganor and V. Gladstein, "The effects of desert particles with sulphate on rain formation in the Eastern Mediterranean", J. Appl. Meteorol., 1996

Li-Jones X. and J. M. Prospero, J. Geophys. Res. 103, 16073, 1998

Mélin F., B. Bulgarelli, N. Gobron, B. Pinty, and R. Tacchi, "An integrated tool for SeaWiFS operational processing", Report of the European Commission EUR 19576 EN, 2000

Molinari E., "Mineralogical characterisation of Saharan dust with a view to its final destination in Mediterranean sediments", S. Guerzoni and R. Chester (eds.), The impact of desert dust across the Mediterranean, Kluwer Academic Publishers, Netherlands, 153-162, 1996

Moore K. D., K. J. Voss and H. R. Gordon, "Spectral reflectance of whitecaps: instrumentation, calibration, and performance in costal waters", J. Atmos. Ocean. Tech. 15, 496-509, 1998

Prospero J. M., I. Olmez and M. Ames, "Al and Fe in PM 2.5 suspended particles in south-central Florida: the impact of the long range transport of African mineral dust", Water, Air and Soil pollution 125, 291-317, 2001

Shettle E. P. and R. W. Fenn, "Models of the aerosols of the lower atmosphere and the effects of humidity variations on their optical properties", Air Force Geophysical Laboratory, Techical Report 0214, Hanscom Air Force Base, Massachusetts, 1979

Shutz L. W., P. Buat-Bernard, R. A. C. Carvalho, A. Cruzado, J. M. Prospero, R. Harriss, N. Z. Heidam and R. Jaenicke, "Long-range transport of mineral aerosols", Group report, in A. H. Knap and M. S. Kaiser (eds.) The long-range atmospheric transport of natural and contaminant substances, Kluwer Academic Publishers, Dodrecht, Boston, London, 197-229, 1990

Tanré D., C. Deroo, P. Duhaut, M. Herman, J. Morcrette, J. Perbos and P. Y. Deschamps, "Description of a computer code to simulate the satellite signal in the polar spectrum : 5S code", Int. J. Remote Sens. 11, 659-668, 1990

Tegen I., P. Hollrig, M. Chin, I. Fung, D. Jacob and J. Penner, J. Geophys. Res. 102, 23895, 1997

Tegen I. and A. A. Lacis, "Modelling of particles size distribution and its influence on the radiative properties of mineral dust aerosol", J. Geophys. Res. 101, 19237-19244, 1996

Acknowledgments

The authors would like to thank Frederic Mélin (Joint Research Centre, Inland and Marine Water Unit) for the providing of the REMBRANDT processing and his help during this work and Richard Santer (Université du Littoral Côte d'Opale, Wimereux, France) for the providing of the radiative transfer code.

Figures

Figure 1: SeaWiFS true-colour browse images from the HROM station: a) fine dust particles event in the middle of clouds across the Mediterranean Sea on October 13, 2000 – b) thick dust storm emitted from Lybia on April 13, 2001.

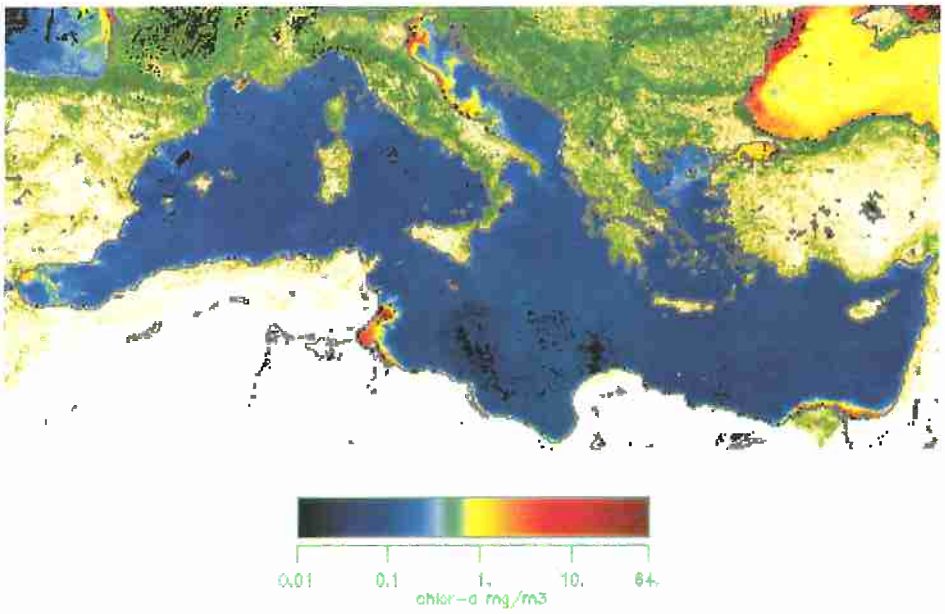

Figure 2: Map of the mean chlorophyll concentration derived with the REMBRANDT code in the Mediterranean Sea. Average on a ten-days basis: from 21/09/1999 to 30/09/1999.

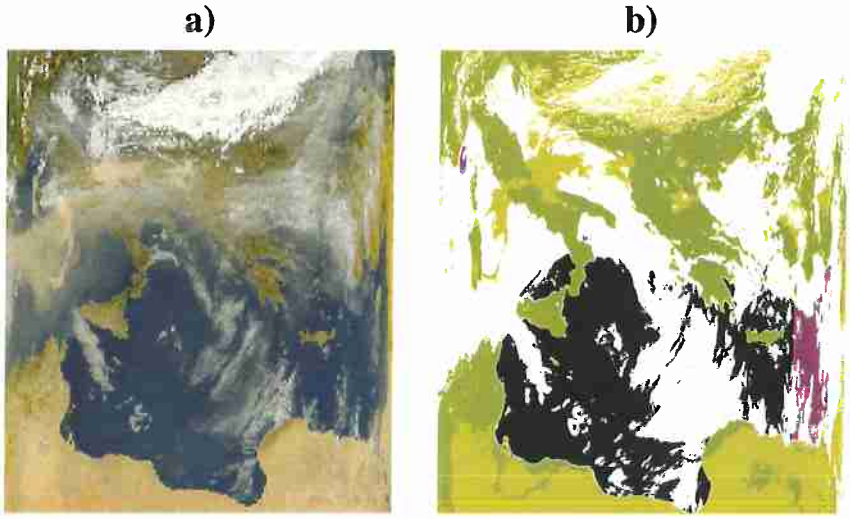

Figure 3: Illustration of dust flagging using the REMBRANDT processing: a) SeaWiFS true-colour browse image from the HSPZ station on October 27, 1999 – b) SeaWiFS flag product for the same day using the REMBRANDT code: green stands for land or very bright surfaces (with albedo greater than a given threshold), white stands for clouds (or dust events), violet stands for bad geometrical conditions pixels and black for non-flagged ones.

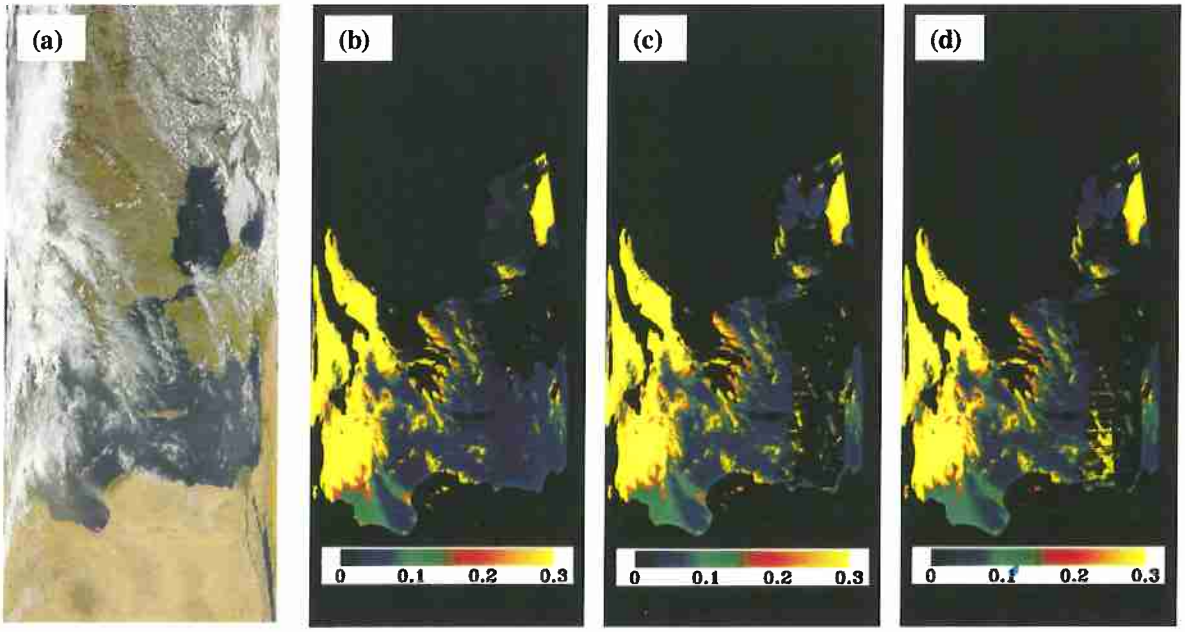

Figure 4: Spectral behaviour of dust aerosol reflectance on April 16, 1999: a) SeaWiFS true-colour browse image from the HSPZ station – b) aerosol reflectance at 865 nm – c) aerosol reflectance at 510 nm – d) aerosol reflectance at 443 nm.

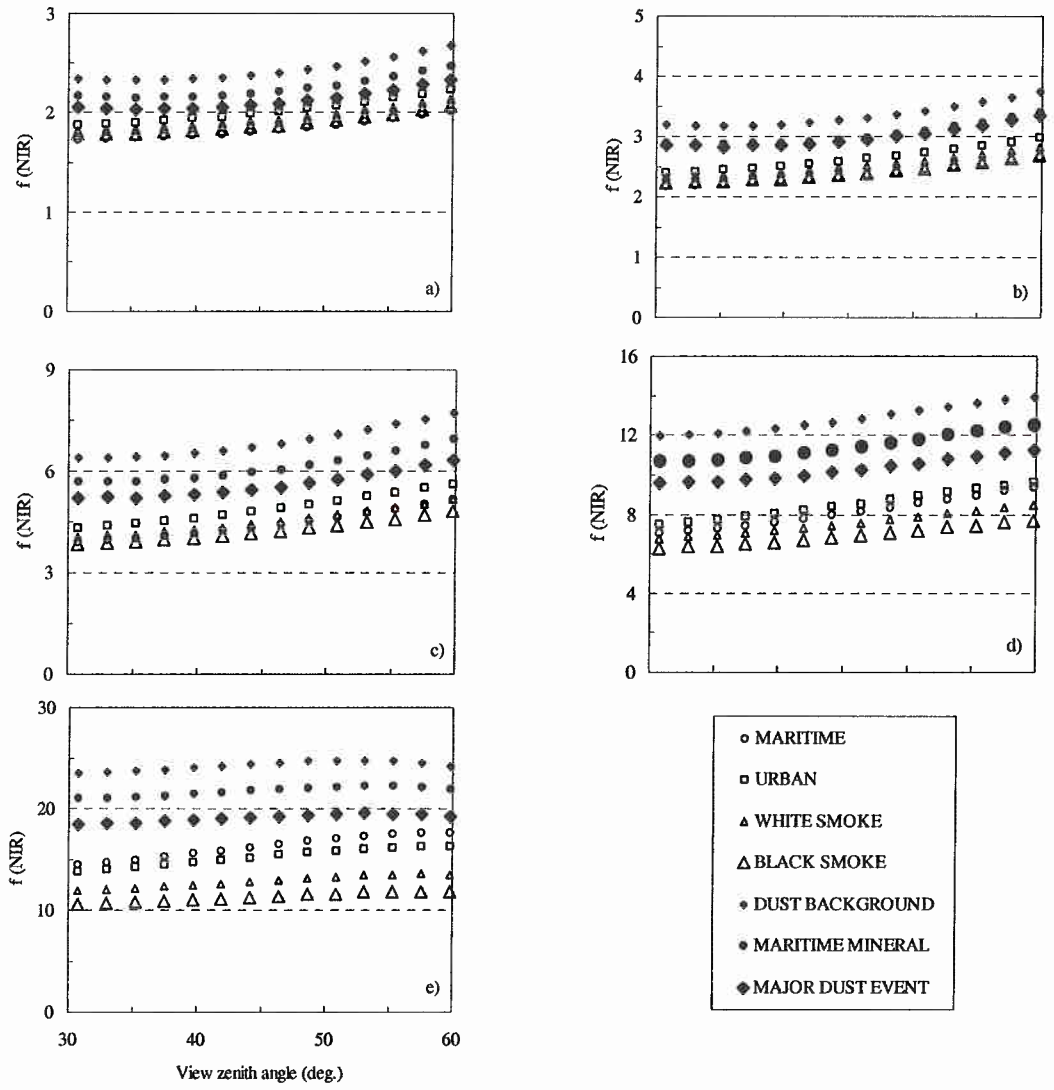

Figure 5: Simulations of the f-ratio at 865 nm for a solar zenith angle of 30°, 7 aerosol models, and 5 visibilities: a) 50 km – b) 23 km – c) 8 km – d) 4 km – e) 2 km.

Figure 6: Study of a transect, drawn in red, along a dust event on April 10, 2000. Flags result from the new REMBRANDT processing.

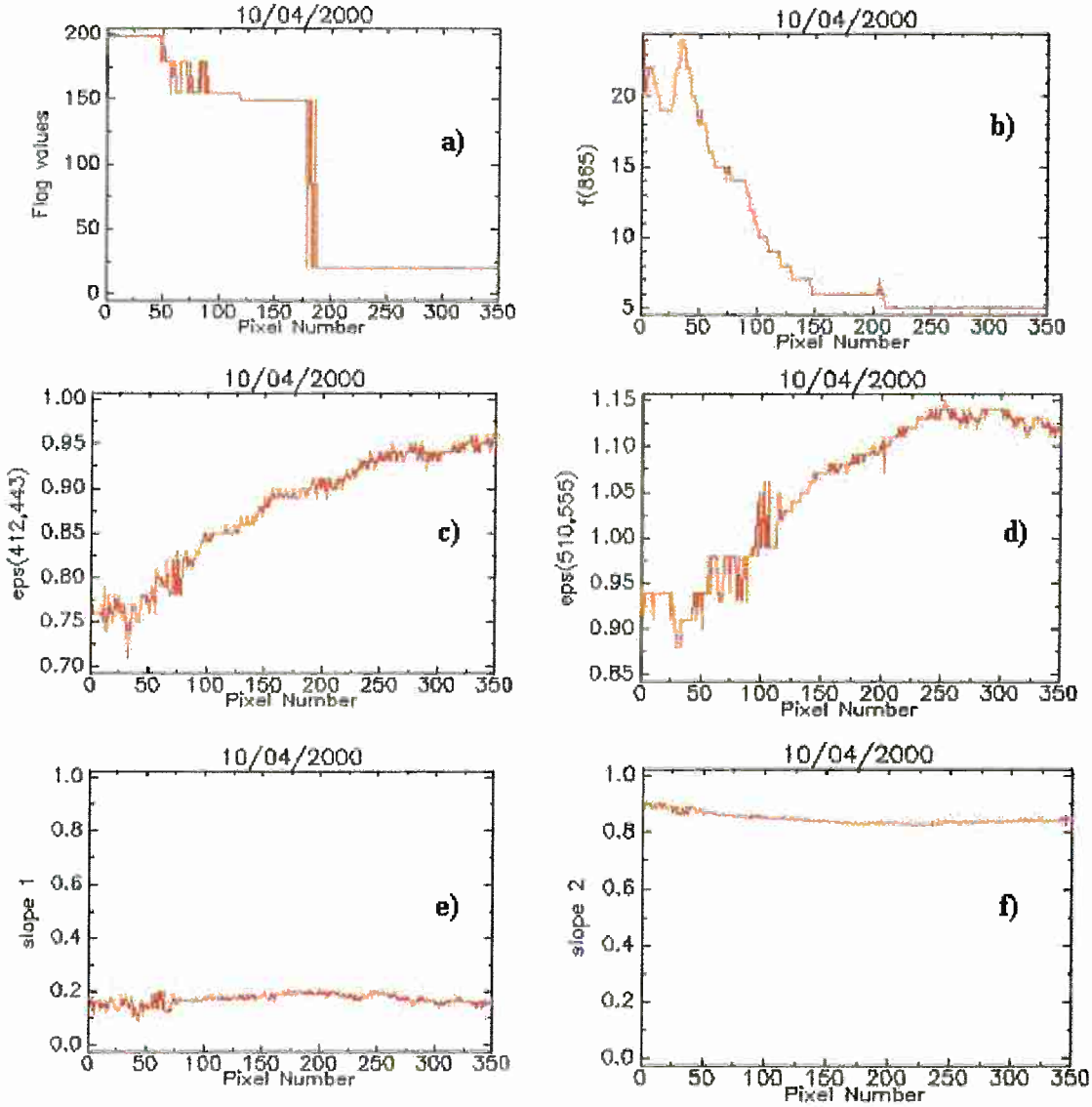

Figure 7: Along the transect represented in Figure 6: a) f(865) – b) ε'(412,443) – c) ε'(510,550) – d) β_s – e) β_l.
For this day, the 4 categories of dust are represented: in Figure a, 199 corresponds to "Dust Storm with Large Particles", 179 to "Major Dust with Large Particles", 155 to "Major Dust with Fine particles" and 149 to "Minor Dust with Fine particles".

Figure 8: Same as Figure 6 for October 5, 2000.

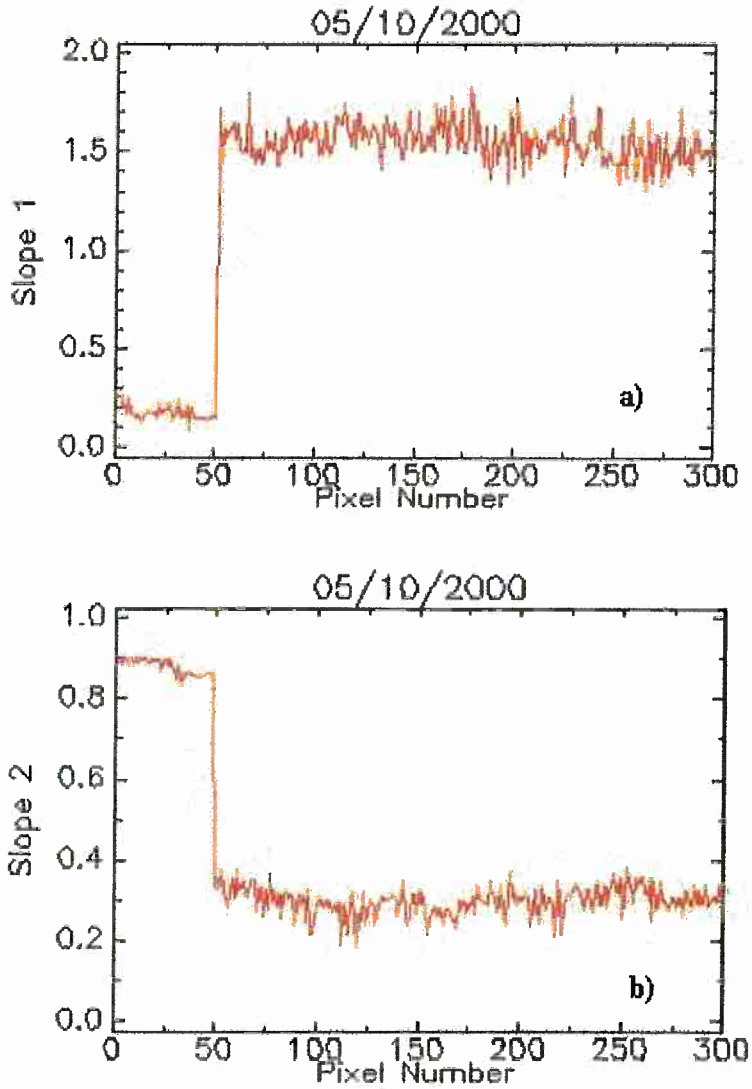

Figure 9: Along the transect represented in Figure 8: a) slope at short wavelengths : β_s – b) slope at long wavelengths : β_l .

Figure 10: New pixel classification for the SeaWiFS data: a) True-colour browse image from the HROM station on April 17, 2001 – b) Corresponding new pixel classification. Land is represented in dark green, clouds in white, "Dust Storm with Large Particles" in dark pink, "Major Dust with Large Particles" in orange, "Major Dust with Fine Particles" in yellow, "Minor Dust with Fine Particles" in clear green and "Background aerosol" in black.

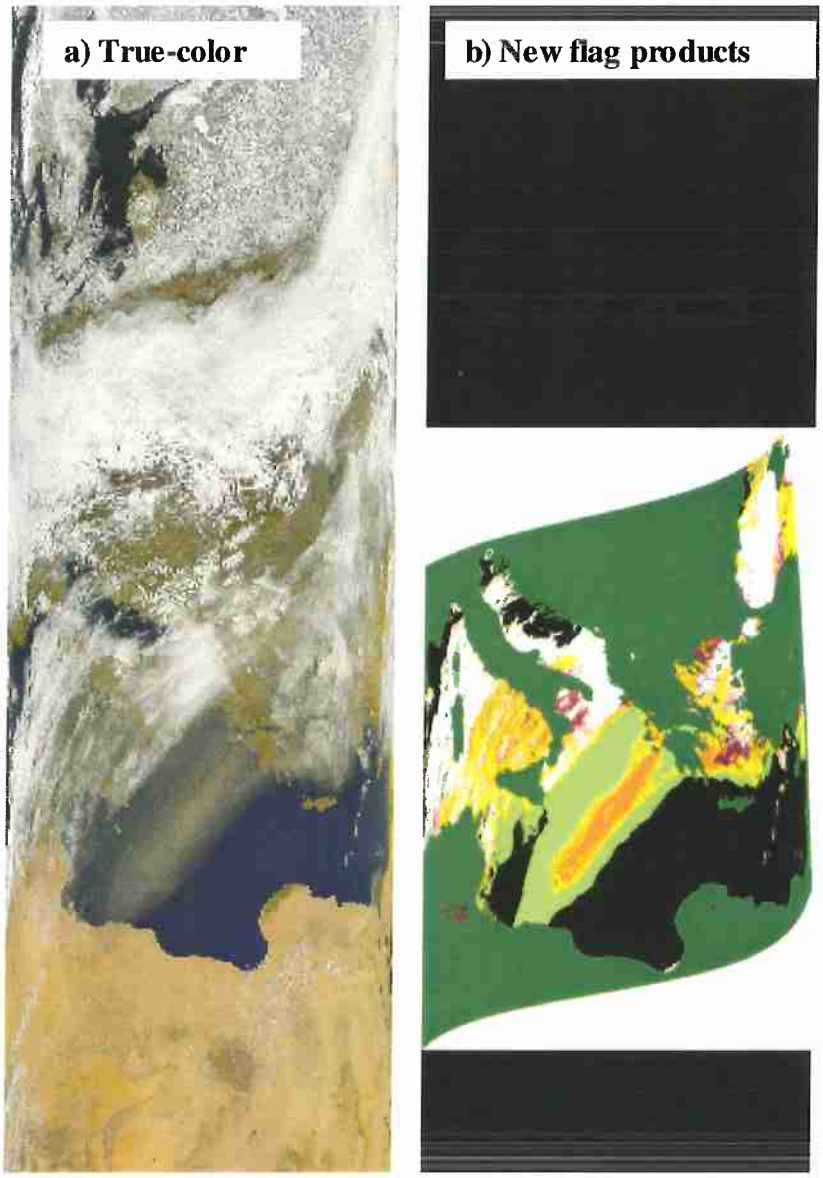

Figure 11: Same as Figure 10 on March 26, 2001, recorded at the HROM station.

Figure 12: Same as Figure 10 on May 30, 1999, recorded at the HSPZ station.

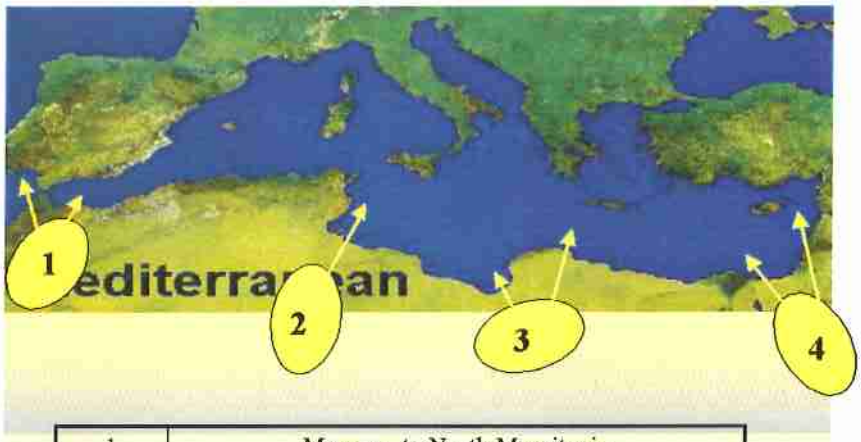

1	Morocco to North Mauritania
2	South Algeria, Mali and Niger
3	South Liban and Chad
4	Egypt and North Sudan

Figure 13: Main sources of Saharan dust particles in the Mediterranean Sea.

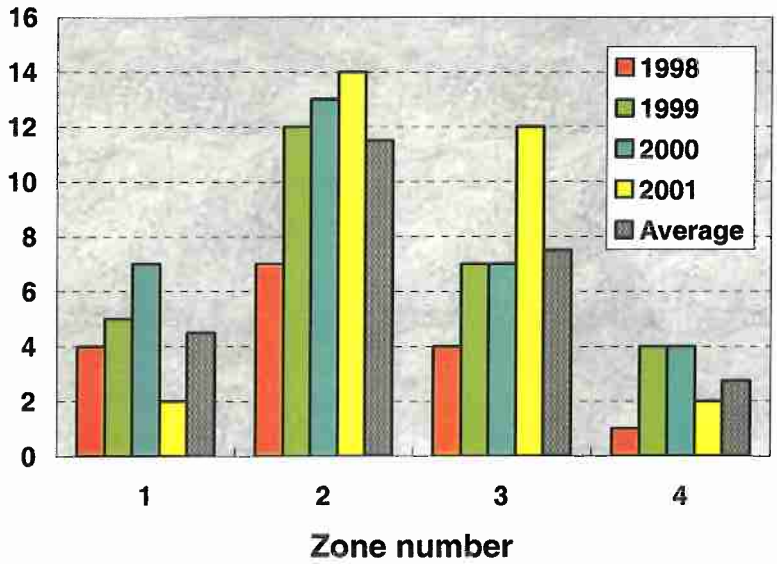

Figure 14: Repartition of the dust events per source for the 1998-2001 period. Zones are detailed in Figure 13.

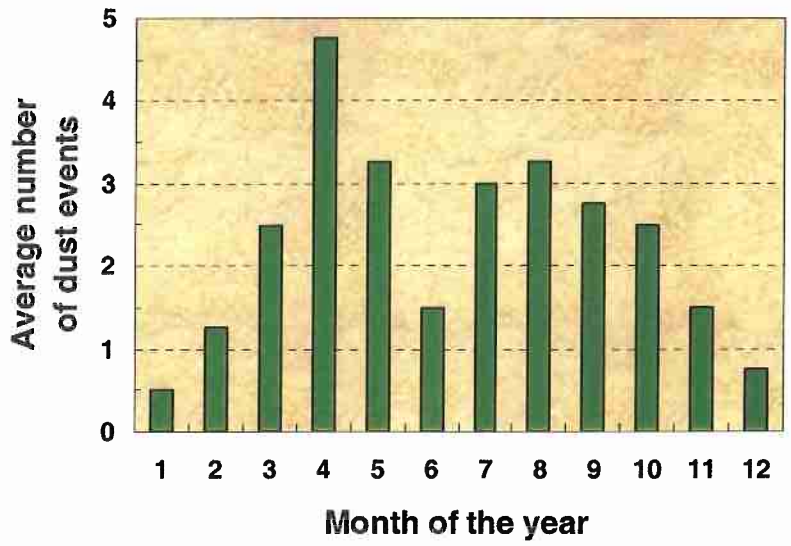

Figure 15: Averaged number of dust events in the Mediterranean Sea for each month of the year.

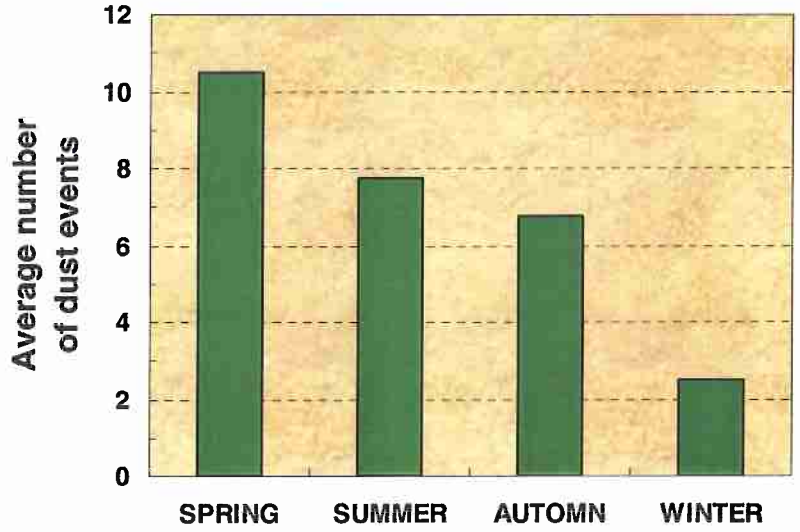

Figure 16: Averaged number of dust events in the Mediterranean Sea per season. March-April-May is the Spring period, June-July-August the Summer, September-October-November the Autumn and December-January-February the Winter.

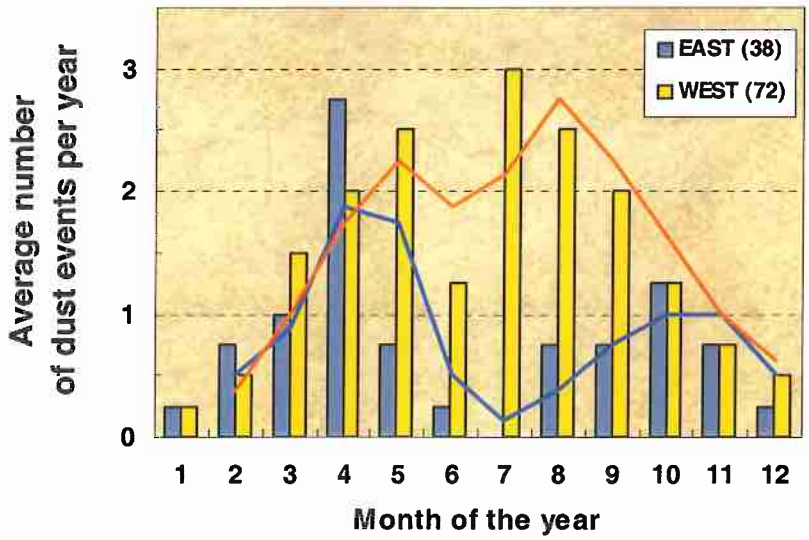

Figure 17: Averaged number of dust events in the Mediterranean Sea for each month of the year. East corresponds to dust produced from sources 1 and 2, West to sources 3 and 4. The total number of events is specified for East (38) and West (72) and the tendency curves are respectively represented in blue and orange.

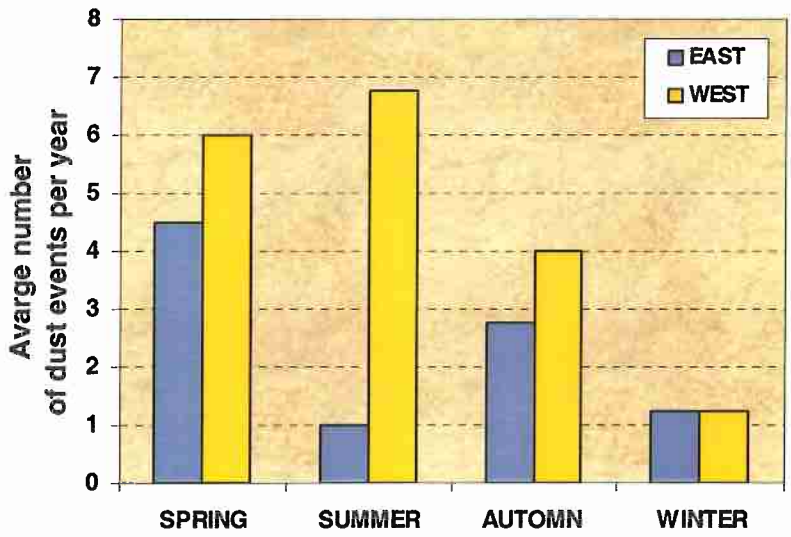

Figure 18: Seasonal averaged number of dust events for East and West sources.

Tables

Number	Aerosol model	Components	Mixing Ratio (%)	References
1	Maritime	Sea-salt (nuc.) Sulfate -	61.5 38.5 -	Shettle & Fenn, 1979
2	Urban	Water-soluble Soot Dust-like	59.45 40.55 0.0000167	D'Almeida, 1991
3	White Smoke	Water-soluble Soot Dust-like	94.0 5.95 0.05	D'Almeida, 1991 Kaufman et al., 2002
4	Black Smoke	Water-soluble Soot Dust-like	94.0 5.9 0.1	D'Almeida, 1991 Kaufman et al., 2002
5	Background dust	Mineral (nuc.) Mineral (acc.) Mineral (coa.)	92.74 7.16 0.0097	D'Almeida, 1991
6	Maritime Mineral	Sea-salt (nuc.) Sulfate Mineral (nuc.)	66.7 29.0 4.3	D'Almeida, 1991
7	Wind Carrying Dust	Mineral (nuc.) Mineral (acc.) Mineral (coa.)	85.42 14.58 0.0073	D'Almeida, 1991

Table 1: Characteristics of aerosol models used for the simulations of f(NIR) in Figure 5.

Category	ε'(412,443)	ε'(510,555)	β_s	β_l
1	≤0.9	≤0.97	0-2.5	Close to 0
2	≤0.9	0.97-1.06	0-3.5	0-1

Table 2: The ε' spectral behaviour highlights 2 categories of dust particles.

Class	f(865)	ε'(412,443)	ε'(510,555)	β_s	β_l	Aerosol Type
1a	≥20	≤0.9	≤0.97	0-2.5	Close to 0	Dust Storm with Large Particles
1b	8-20	≤0.9	≤0.97	0-2.5	Close to 0	Major Dust event with Large Particles
2a	8-20	≤0.9	0.97-1.06	0-3.5	0-1	Major Dust event with Fine Particles
2b	3-8	≤0.9	0.97-1.06	0-3.5	0-1	Minor Dust event with Fine Particles
3	≤3	>1	>1	$\lvert \beta_s - \beta_{sD} \rvert > 0.5$	$\lvert \beta_l - \beta_{lD} \rvert > 0.3$	No dust event (background aerosol conc.)

Table 3: The new pixel classification includes 5 classes of aerosols.

Mission of the JRC

The mission of the JRC is to provide customer-driven scientific and technical support for the conception, development, implementation and monitoring of EU policies. As a service of the European Commission, the JRC functions as a reference centre of science and technology for the Union. Close to the policy-making process, it serves the common interest of the Member States, while being independent of special interests, whether private or national.

EUROPEAN COMMISSION
JOINT RESEARCH CENTRE